Journal of Applied Sciences

ISSN 1812-5654

science alert

ANSInet
an open access publisher
http://ansinet.com

Journal of Applied Sciences 9 (7): 1238-1247, 2009
ISSN 1812-5654

Variability of Clays from Gounioube Deposit (Ivory Coast)

[1]J.Y.Y. Andji, [1]A. Abba Toure, [1]G. Kra and [2]J. Yvon
[1]Laboratoire de Chimie des Matériaux Inorganiques, Université de Cocody,
22 BP 582 Abidjan 22, Côte d'Ivoire
[2]Laboratoire Environnement Minéralurgie, UMR CNRS-INPL 7569 Nancy Université,
15 Avenue du Charmois, BP 40 F-54501, Vandoeuvre lès Nancy Cedex, France

Abstract: The aim of this study is to estimate, from the statistics (PCA), the variability of the clays from the deposit of Gounioube, in order to choose the different grades convenient for a given application and eventually correct the defective ones. Indeed, most of industrial minerals are used in fields where benefit is taken from variable properties that, directly or not, govern their applications. So, fourteen samples of kaolin clays from Gounioubé deposit (Ivory Coast), have been studied by chemical, crystallographic (X-Ray Diffraction (XRD)), spectroscopic (IR, UV, EPR), particle size and textural analysis.

Key words: Kaolinite, X-Ray diffraction, IR, UV, EPR, TEM, fineness, PCA

INTRODUCTION

Kaolin is a major industrial mineral used in very diversified applications (papers, polymers, ceramics, cosmetics, drugs). Though the production countries are significantly changing these last years (mainly Brazil) and paying account of ambiguous definitions, the annual world output of based on kaolinite materials is stable and estimated to 45 millions of metric tons (USGS, 2008).

The beneficiation of these materials in each domain needs to know and understand the links between intrinsic physicochemical properties of the material and their macroscopic behaviours. In addition, any one that try to transform a raw material needs to know as early as possible in the time and in the upstream of the process, what are the best raw materials and the most convenient process leading to optimal service aptitudes of the final grades. Initially, this approach does not consider how the mechanisms by which the properties of components or the processing conditions rule the final efficiency of the composite, but it defines a set of ranking criteria that lead to evaluate what quality of mineral can enter under satisfying conditions in what compound, paying account of specific conditions (Yvon *et al*., 2002). At last, the efficiency of developing trials in countries where the applications of the mineral industry are not still integrated into the economic activity need to avoid a strict copy of products used in northern markets, but for being successful have to develop products adapted to local conditions.

This study aims at evaluating the variability of the Gounioubé deposit based upon the knowledge of the specific mineralogy, crystal-chemistry and physical-chemistry of kaolins from this deposit, in connection with their possible uses.

MATERIALS AND METHODS

Location and geology of the deposit: Kaolins samples have been collected on the Gounioubé deposit (City of Anyama, Ivory Coast). The field is mainly out of a detrital sandy-clay plateau from the terminal continental level (miocene-pliocene), resulting from a ferallitic alteration of the basal rocks under humid tropical climate (Dorthe, 1964).

Methods: Fourteen samples have been collected in different pits, at different depth of the deposit of Gounioube, a city located at 30 km from Abidjan in the south of Côte d'Ivoire (Andji, 1998). The samples have been 5 sec ground at 1400 rpm in a cylinder mill until obtaining less than 3 mm fractions. After that, they have been homogenised and quartered into 50 g specimens. The specimens were dispersed in 1.5 L of ultra pure water using a 520 rpm rotative stirrer until homogenisation of the suspension. The initial pH, close to 5, was increased at 9 with ammonia. The suspension was then decanted and sieved at 30 μm. The fine fractions were submitted to chemical, crystallographic and spectroscopic, Infra Red (IR) and Ultra Violet (UV), Electron Paramagnetic

Corresponding Author: J.Y.Y. Andji, Laboratoire de Chimie des Matériaux Inorganiques, Université de Cocody,
22 BP 582 Abidjan 22, Côte d'Ivoire

Resonance (EPR), analysis; microscopic determinations were carried out using Transmission Electron Microscopy (TEM); particle size determination and measurement of specific surfaces were also determined.

Chemical analysis were obtained at the Centre de Recherches Pétrographiques et Géochimiques (Nancy, France) by Inductively Coupled Plasma-Atomic Emission Spectroscopy (ICP-AES) for major elements and Inductively Coupled Plasma-Mass Spectroscopy (ICP-MS) for trace elements, after fusion with $LiBO_2$ and dissolution in HNO_3. Analytical conditions and limits of detection are found by Carignan *et al.* (2001).

Sulphur is oxidized into sulphuric acid in an induction furnace and then titrated by impulse coulometry using an Hermann-Moritz device. The relative preciseness reaches 5% around 0.3% S and 20% around 0.01% S.

Structure water H_2O^+ and hydration water H_2O^- were titrated according to Penfield's method.

X-Ray Diffraction (XRD) analyses were carried out using the following devices and procedures:

- Disoriented powder diffraction diagrams were obtained using a Jobin-Yvon Sigma 2080 diffractometer working by reflection using the copper $K\alpha_1$ radiation. Oriented preparations were analysed by reflection with a Bruker D8 device using the cobalt $K\alpha_1$ radiation

Disoriented total rock diffractometry: The diffractograms show the whole set of (hkl) reflections of kaolinite and associated minerals, mainly quartz, micas and anatase (Fig. 1). The crystal defects lead to variations of the (hkl) profile lines. Here, R1 and R2 indexes (Table 1) according to Liétard (1977) have been used, they measure the amount of random defects in the (a, b) plane.

Diffractograms on oriented preparations: The X-ray diffractometry on oriented preparations allowed us to measure the angular width at half intensity of the (00l) line of kaolinite, in order to deduce the coherent scattering thickness (Table 1) along the c axis that measures the packing order according to Scherrer (1918).

The absorption spectra are carried out in the field of the mean infrared, that is to say for numbers of wave ranging between 400 and 4000 cm^{-1} (Fig. 2).

The half cell of kaolinite contains four hydroxyl groups the O-H stretching vibration of which are revealed by four absorption bands at 3655, 3670, 3695 cm^{-1} for external OH and at 3620 cm^{-1}, for internal OH (Farmer, 1964). The bending vibrations of the Al-OH group are revealed by a large band centred around 915 cm^{-1} with a shoulder at 938 cm^{-1} on its high frequency side.

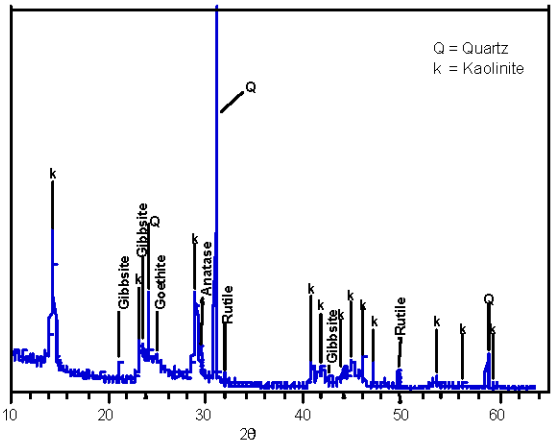

Fig. 1: Example of diffractograms obtained (sample G14)

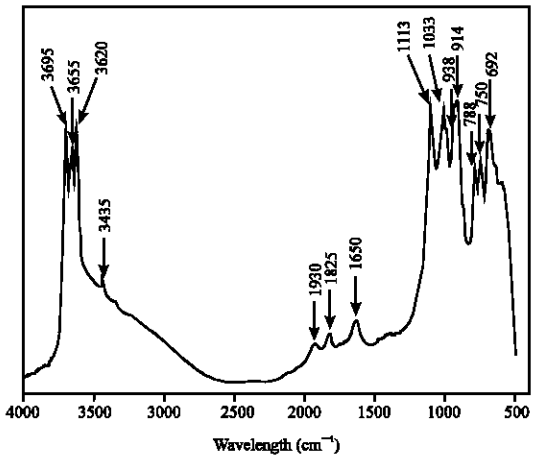

Fig. 2: Example of infrared spectra obtained (sample G9)

Table 1: Cristallinity indexes

Samples	R1	R2	DC (001)	P1	P2
G1	-	-	143	-10×10^{-4}	0.758
G2	0.90	0.98	135	-42×10^{-4}	0.806
G3	0.58	1.09	119	-16×10^{-4}	0.715
G4	0.65	1.08	119	-19×10^{-4}	0.762
G5	0.48	0.81	149	-17×10^{-4}	0.745
G6	0.92	0.66	132	-33×10^{-4}	0.772
G7	0.75	0.65	132	-29×10^{-4}	0.791
G8	-	-	140	-33×10^{-4}	0.769
G9	0.67	1.07	163	-49×10^{-4}	0.823
G10	0.76	1.05	145	-6×10^{-4}	0.765
G11	-	-	132	-13×10^{-4}	0.776
G12	-	-	132	-7×10^{-4}	0.691
G13	-	-	119	-20×10^{-4}	0.720
G14	0.55	0.68	140	-33×10^{-4}	0.758

For evaluating the crystal order, the two index P1 and P2 defined by Liétard (1977) and Cases *et al.* (1982), have been used (Table 1). P1 is the slope of the segment joining the band at 938 cm^{-1} to the band at 915 cm^{-1}; a positive slope reveals a well defined band, a negative one reveals

a simple shoulder. P2 is the ratio between the 3672 and the 3655 cm^{-1} bands; this ratio is slightly lower to 1 for well ordered kaolinites and growths with the number of defects. The spectra have been recorded in transmission or diffuse reflectance mode, using an IFS55 Bruker device with a usual spectral resolution of 2 cm^{-1}.

A double beam spectrometer equipped with an integration sphere has been used (Shimadsu UV 2100) working in visible and ultra violet (800-200 nm), on slightly pressed powders. The spectroscopic data allow to calculate the conventional parameters L*, a* and b*. These data respectively correspond to white-black, red-green and blue-yellow axis that allows to place the samples in the trichromatic space, the calculation are carried out according to the usual wave lengths 458, 570 and 770 nm. Their formulas are as follows:

$$L^* = 116\,(\text{Green filter absorbance}/100)^{1/3} - 16$$

$$a^* = 500\,[(\text{Red filter absorbance}/100)^{1/3} - (\text{green filter absorbance}/100)^{1/3}]$$

$$b^* = 200\,[(\text{Green filter absorbance}/100)^{1/3} - (\text{blue filter absorbance}/100)^{1/3}]$$

IB, IJ and Eab* parameters, respectively represent brightness, yellow index and the difference between the pure white (L* = 100, a* = 0, b* = 0) they have been calculated using the usual following formulas:

$$IB = (4\times\text{Blue filter aborption}) - (3\times\text{Green filter absorption})$$

$$IJ = (128\,X - 106\,Z)/Y$$

$$Eab^* = [(L^*-100)^2 + (a^*-100)^2 + (b^*-100)^2]$$

where, X, Y and Z are three chromatic coordinates, respectively measuring the red, green and blue colour, of the materials.

The specific surfaces (Table 2) have been deduced of the 77 K nitrogen adsorption isotherms, according to the usual BET method (Brunauer *et al*., 1938). The adsorbometer is a conventional step by step volumetric device built by LEM (Nguetnkam *et al*., 2005). The samples were outgased under a residual pressure of 10^{-4} Pa for 18 h at 110°C.

The particle size analysis (Table 3) has been determined by laser diffraction using a Malven Mastersizer MS 20 device operating from 0.1 to 600 μm, the particle size distributions lead to the passing sizes at 90, 75, 50 and 25%, respectively corresponding to d_{90}, d_{75}, d_{50} and d_{25} values.

Table 2: Specific surfaces (BET) and Cation Exchange Capacity (CEC)

Samples	BET surfaces ($m^2\ g^{-1}$)	CEC (meq/100 g)
G1	51.83	9.27
G2	48.73	8.52
G3	43.87	7.68
G4	42.85	7.00
G5	51.83	11.00
G6	59.28	11.34
G7	54.10	9.18
G8	47.80	8.69
G9	38.22	7.13
G10	50.78	11.29
G11	50.60	10.11
G12	49.94	9.62
G13	52.84	7.50
G14	44.51	10.37

Table 3: Particle size analysis (μm)

Samples	d_{90}	d_{75}	d_{50}	d_{25}
G1	06.10097	4.12961	2.43282	1.34048
G2	13.6153	7.58279	3.16724	1.38355
G3	19.9051	12.23210	5.50637	2.13842
G4	17.3701	9.26776	3.53979	1.55497
G5	17.4705	10.00930	4.28165	1.88801
G6	19.1381	11.28650	4.97312	2.10358
G7	20.2961	12.38850	5.39000	2.11190
G8	20.5142	12.93900	5.90206	2.32058
G9	16.0086	8.87839	4.26556	2.07408
G10	16.0438	8.85702	3.92992	1.81711
G11	13.9071	8.50814	4.04101	1.80383
G12	18.7688	11.80270	5.64202	2.35136
G13	28.8924	18.12370	8.58145	2.48969
G14	03.86892	2.91830	1.96250	1.16351

The cation exchange capacity of a clay material (Table 2) is the number of equivalent positive charge for neutralizing its negative charge at pH 7. It has been determined by deplacing the compensating cations using cobalt-hexammonium ($Co[(NH_3)_6]^{3+}$) cation according to the method developed by Mantin and Glaeser (1960) and Rémy and Orsini (1976). The exchanged species have also been titrated in the exchange solution.

The different phases of the materials were determined by Energy Dispersive Spectroscopy (EDS) using a Philips SM 20 transmission microscope working at 200 kV and equipped with a PGT model EDS with ultra thin windows. Samples have been sonicated in ethanol, sampled as a drop and spread on a copper supported carbon grid.

The fundamentals of calculation used here for determining the quantitative mineralogy of specimens are completely described by Yvon *et al*. (1990a, b). The vector of the elementary composition (CHIMe) of a mixture of minerals can be described as the product of a nominal amount matrix (STOEC) by a vector of the phase amounts (X), then:

$$CHIMe = STOEC\times X$$

This equation admits a less square solution as:

$$Xe = (STOEC^T\times STOEC)^{-1}\times STOEC^T\times CHIMe$$

where, $STOEC^T$ is the STOEC transposed matrix. One can appreciate the quality of the determination by calculating the residues based on :

$$CHIM = STOEC \times Xe$$

With the absolute residue

$$«Residue» = CHIM - CHIMe$$

If the residue coordinates are positive or close to zero and if the mineralogical composition is in qualitative agreement with the other analyses, (DRX, DRIFTS,), then the determination is considered as valid.

The whole set of data has been processed through normalized Principal Component Analysis according to Lebart *et al*. (1979).

RESULTS AND DISCUSSION

Nature of phases and associated elements: A preliminary evaluation of the Gounioubé deposit (Andji *et al*., 2001), using conventional methods revealed that the coarser fractions of the crude material are out of kaolinite associated to quartz, potassic feldspars, maghemite, gœthite, rutile, illite, gibbsite and small quantities of phosphoferrite.

For evaluating the variability of beneficiable fractions, the crude ore was sieved at 30 µm the chemical analysis (Table 4, 5) and mineralogical determination (Table 6) of this fraction were carried on. In addition, the illite composition was determined by TEM/EDS analysis that also, revealed the presence of swelling clays (Fig. 3a, b).

Quantitative mineralogy: Kaolinite, quartz, anatase and/or rutile and iron oxy-hydroxydes, are revealed by XRD and DRITF spectroscopy. Both these techniques give also a semi-quantitative evaluation of the mixture and identify small amounts of gibbsite.

CBD treatment (Table 7), shows that most of the iron contained in Gounioubé materials is included in iron minerals, intimately associated with kaolinite what is a usual occurrence (Hogg *et al*., 1975; Delineau, 1994; Delineau *et al*., 1994). Then we shall consider the octahedral iron evaluated through ESR after CBD

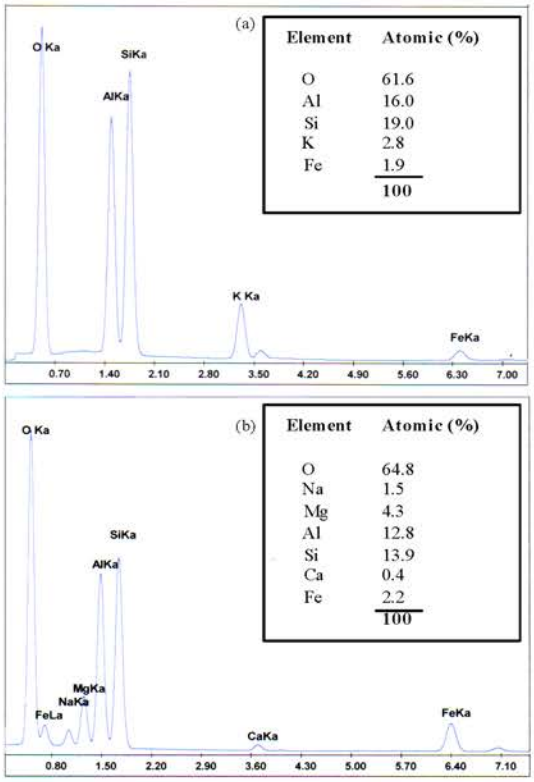

Fig. 3: Transmission electron microscopy/energy dispersive spectrometry, (a) of a cristal of illite in G9 and (b) of a smectite clay in G13

Table 4: Chemical analysis of fraction at 30 µm: percentages of major elements

Samples	SiO_2	Al_2O_3	Fe_2O_3	MnO	MgO	CaO	Na_2O	K_2O	TiO_2	P_2O_5	PF	Total	H_2O^+	H_2O^-	S-tot
G1	47.39	32.35	3.18	-	0.29	-	-	0.36	2.76	0.39	13.05	99.77	11.96	1.61	0.036
G2	44.43	35.98	1.97	-	0.21	0.20	-	0.31	2.69	0.34	13.75	99.88	13.14	1.68	0.027
G3	43.44	37.34	1.61	-	0.12	0.13	-	0.23	2.65	0.36	14.01	99.89	13.56	1.26	0.035
G4	43.21	37.45	1.43	-	0.11	0.17	-	0.17	2.88	0.37	14.12	99.91	13.62	1.20	0.029
G5	46.53	32.50	3.44	-	0.28	0.24	0.05	0.38	2.78	0.50	13.23	99.93	12.18	1.76	0.040
G6	41.99	33.66	6.52	-	0.22	0.23	-	0.30	2.51	0.55	13.90	99.88	12.86	1.97	0.032
G7	42.50	35.69	3.93	-	0.19	0.22	-	0.28	2.61	0.42	14.07	99.91	13.19	1.59	0.026
G8	42.98	36.89	2.29	-	0.17	0.23	-	0.26	2.61	0.38	14.07	99.88	13.45	1.47	0.032
G9	43.27	37.71	1.67	-	0.15	0.21	-	0.24	2.18	0.42	14.07	99.92	13.64	1.20	0.036
G10	48.04	31.81	3.00	-	0.33	0.30	0.05	0.34	2.67	0.41	12.95	99.91	11.87	1.95	0.042
G11	46.70	33.75	2.13	-	0.28	0.25	-	0.37	2.89	0.34	13.17	99.88	12.24	1.78	0.032
G12	44.57	35.78	1.76	-	0.22	0.25	-	0.33	2.83	0.31	13.85	99.90	12.93	1.56	0.029
G13	33.11	31.46	18.27	-	0.15	0.13	-	0.16	2.27	0.29	14.04	99.88	13.21	1.41	0.041
G14	41.43	37.38	3.30	-	0.18	0.27	-	0.21	2.36	0.55	14.31	99.99	13.83	1.35	0.035

Table 5: Chemical analysis of fraction at 30 µm

ECH	G1	G2	G3	G4	G5	G6	G7	G8	G9	G10	G11	G12	G13
As	4.31	3.39	3.33	4.01	3.64	3.95	3.05	3.69	2.67	5.49	3.61	2.71	28.6
Ba	202	224	206	232	224	246	274	235	268	202	250	227	110
Be	1.58	1.67	<Id	<Id	<Id	<Id	<Id	<Id	<Id	<Id	1.63	1.51	<Id
Bi	1.16	1.11	1.05	1.29	0.97	0.84	1.26	1.11	1.06	0.87	1.05	0.96	0.94
Cd	0.50	0.89	0.34	0.30	0.46	<Id	0.43	0.35	<Id	<Id	<Id	<Id	<Id
Ce	2.10	230	218	218	205	205	225	222	216	189	239	216	168
Co	4.76	4.57	3.55	3.54	4.85	4.54	4.80	3.74	4.34	4.46	4.74	4.10	3.27
Cr	242	267	274	323	287	292	358	444	660	213	245	240	288
Cs	4.88	3.65	2.71	2.09	4.17	3.35	2.79	2.84	1.77	4.29	4.17	3.14	1.89
Cu	53.9	64.4	57.00	82.4	61.0	72.8	63.5	67.5	52.8	79.5	68.2	105	72.4
Dy	7.04	7.75	7.21	8.12	7.77	8.91	9.58	9.67	9.73	7.80	9.87	8.83	4.57
Er	4.45	4.48	4.18	4.38	4.87	4.14	4.65	4.74	4.43	4.32	4.90	4.19	2.44
Eu	2.45	2.85	2.68	2.60	2.65	2.77	3.22	3.16	3.24	2.34	3.05	2.75	1.54
Ga	54.7	69.8	62.4	71.7	52.8	59.1	73.8	61.2	78.2	55.5	68.6	63.6	54.3
Gd	9.33	9.71	9.81	9.04	10.6	10.4	11.4	11.5	12.0	9.37	10.6	9.11	4.88
Ge	2.12	2.53	1.91	2.06	2.15	2.23	2.34	2.14	2.72	2.06	2.63	2.03	1.69
Hf	21	18.2	17.6	21.9	19.8	16.7	22.7	20.8	19.0	20.7	23.5	19.3	15.3
Ho	1.55	1.59	1.48	1.53	1.69	1.64	1.73	1.74	1.69	1.55	1.89	1.63	0.866
In	0.19	0.17	0.21	0.25	0.20	0.16	0.20	0.24	0.33	0.16	0.20	0.20	0.16
La	106	123	112	120	100	115	118	116	104	103	130	119	97.3
Lu	0.702	0.712	0.601	0.696	0.674	0.630	0.649	0.655	0.565	0.717	0.800	0.745	0.442
Mo	3.38	3.28	3.14	3.04	2.90	3.24	3.45	3.03	2.59	3.61	4.12	3.43	9.52
Nb	71.6	73.00	67.3	79.8	68.3	60.7	70.2	69.9	54.8	64.1	76.1	68.0	56.5
Nd	69.4	76.3	69.00	76.5	74.2	83.5	88.5	85.4	82.2	70.4	92.0	85.0	53.4
Ni	54.7	50.2	42.5	41.0	51.1	45.7	48.5	49.3	48.7	45.4	48.5	43.4	27.3
Pb	52.2	63.4	57.8	64.6	53.7	55.2	63.4	60.7	58.5	51.1	65.7	59.6	52.3
Pr	23.1	24.4	22.9	23.7	23.3	22.3	25.6	25.0	23.3	21.0	26.3	22.7	17.0
Rb	36.3	29.6	18.8	14.7	29.7	28.3	25.7	20.3	17.0	32.5	33.9	24.8	13.2
Sb	0.80	0.79	0.66	0.90	0.68	0.87	1.16	0.97	1.26	0.72	1.01	0.76	0.97
Sm	11.0	13.4	11.7	12.8	12.4	15.2	15.3	15.4	15.2	11.5	14.9	14.2	8.04
Sn	9.03	8.86	8.57	10.9	8.05	7.51	9.72	9.16	8.03	8.38	9.62	8.37	7.38
Sr	224	316	338	434	251	262	276	307	293	206	266	276	119
Ta	5.66	5.82	5.35	6.58	5.39	5.04	6.14	5.73	4.80	5.46	6.78	5.78	4.66
Tb	1.31	1.41	1.27	1.40	1.39	1.61	1.71	1.71	1.79	1.34	1.65	1.48	0.772
Th	33.8	39.8	36.8	47.2	37.1	36.9	49.2	44.3	50.5	32.9	41.4	38.0	34.1
Tm	0.652	0.654	0.571	0.678	0.700	0.618	0.681	0.691	0.632	0.646	0.713	0.629	0.404
U	4.97	4.85	3.82	4.81	5.47	5.16	5.86	4.58	5.99	5.03	5.56	4.70	4.07
V	108	111	87.4	94.8	120	128	120	92.6	107	104	112	93.1	246
W	4.54	4.46	4.14	5.24	4.42	4.39	5.51	4.59	4.37	4.84	5.71	5.01	4.06
Y	42.5	40.5	39.7	45.0	45.0	36.7	44.4	46.8	40.0	37.2	43.5	39.3	22.3
Yb	3.98	4.34	3.53	4.64	4.07	4.26	4.51	4.55	4.02	4.23	5.05	4.25	2.67
Zn	101	82.3	67.50	76.8	95.6	81.5	97.9	84.1	83.6	97.1	89.7	82.7	65.5
Zr	807	767	746	895	910	813	904	840	660	921	926	689	645

Minor elements express in ppm

Table 6: Mineralogical determination

Samples	Phases identified different of those of the kaolinite	Reticular distance (Å)
G1	Qz-Ana-Rut.	4,252-3,520-3,340-3,245-2,456-2,281-2,236-2,126-1,979-1,817
G2	Qz-Ana-Carb.	4,247-3,513-3,335-2,931*-1,979-1,817
G3	Qz-Ana-Rut-Sid-Hém.	3,509-3,334-3,239-2,763*-2,684
G4	Qz-Ana-Rut-Gibb.	4,836 - 3,513-3,336-3,242*-1,816
G5	Qz-Ana.	4,249-3,522-3,342-2,455-2,282-2,236-2,126-1,979-1,817
G6	Qz-Ana-Rut.	4,229-3,505-3,328-3,237-2,123-1,977-1,814
G7	Qz-Ana-Rut.	4,252-3,529 - 3,341-1,818
G8	Qz-Mica-Ana-Rut.	4,955 - 3,337-3,241
G9	Qz-Mica-Go.	9,910-4,153-3,328-1,990
G10	Qz-Ana-Rut.	4,257-3,529-3,344-3,247-2,457-2,282-2,235-2,126-1,980-1,818
G11	Qz-Ana-Rut.	4,236-3,513-3,332-3,239-2,454-2,278-2,123-1,975-1,816
G12	Qz-Ana-Rut-Py.	4,233-3,325-3,235 - 1,814
G13	Qz-Go-Ana.	4,883-4,127-3,513-3,335-2,692-2,415-2,159
G14	Qz-Go-Gibb-Ana-Lép-Carb-Rut.	6,244-4,844-4,134-3,517-3,340-3,242-2,983-2,697-1,818

Qz: Quartz, Ana: Anatase, Rut: Rutile, Hém.: Hematite, Gibb: Gibbsite, Go: Goethite, Lép: Lepidocrocite, Sid: Siderite, Py: Pyrite, Carb: Carbonate

treatment for defining the unit cell composition of kaolinite, what leads to the following formula :

$$Si_4 (Al_{3.98} Fe_{0.02}) O_{10} (OH)_8$$

According to the EDS data (Fig. 3) illite and smectites were defined upon the following principles:

$$(Al_{2-x} Fe^{III}_x) (Si_{4-y} Al_y) O_{10} (OH)_2 K_y$$ for illite

$(Al_{2-x-y}\ Fe^{III}_{x}Mg_{y})\ (Si_{4-z}\ Al_{z})\ O_{10}\ (OH)_2\ Na_{y+z-t-u}\ Al_{t/3}\ Ca_{u/2}$ for smectites

What leads to

$(Al_{1.85}\ Fe_{0.15})\ (Si_{3.49}\ Al_{0.51})\ O_{10}\ (OH)_2\ K_{0.51}$ for illite

$(Al_{1.7}\ Fe_{0.1}\ Mg_{0.2})\ (Si_{3.7}\ Al_{0.3})\ O_{10}\ (OH)_2\ Na_{0.06}\ Al_{0.13}\ Ca_{0.03}$ for smectites

Calculation hypothesis

- Gibbsite is free of iron
- Titanium oxides are grouped under the name Anatase
- The fraction of iron which does not belong to major silicates (kaolinite, micas and smectites) and non expressed under the form of gœthite is grouped under the label residual iron, the same for magnesium residual MgO

The stoichiometry matrix (STOECH) that contains the nominal amounts of oxides in minerals is as follows:

	Kaolinite	Quartz	Anatase	Illite	Smectite	Goethite	Gibbsite
Si	0.465	1	0	0.545	0.6	0	0
Al	0.393	0	0	0.313	0.295	0	0.65
Fe	0.003	0	0	0.031	0.02	0.9	0
Mg	0	0	0	0	0.02	0	0
Ca	0	0	0	0	0.005	0	0
K	0	0	0	0.063	0	0	0
Ti	0	0	1	0	0	0	0
PF	0.14	0	0	0.05	0.05	0.10	0.35

Results of quantitative mineralogy: Numerical results are shown in Table 8.

As expected, kaolinite is the major mineral (48.19-81.81%). The amounts in smectites (4.4-11.69%); gibbsite (4.85-11.21%), illite (2.7-6.03%) and gœthite (1.13-19.69%), are not so low that the X-ray diffractometry would suggest; that can result from the fact that quartz disorient the X-ray preparation what leads to minimize the response of basal reflections of minor lamellar species. The residual iron is always positive or equal to zero and the residual H_2O^+ after calculation is always positive what is in agreement with the fact that XRD reveals iron oxyhydroxides identified as goethite (FeOOH).

Statistics: The whole set of numerical data (67 parameters, including: chemical analysis of trace elements, mineralogical composition, order indexes, colour parameters, CEC, particle size and textural characteristics) was processed through Normalized Principal Component Analysis (PCA) (Fig. 4A), this PCA analysis reveals that the variability of the system depends on a large number of parameters, since the four first factors only explain 42.8% of the total inertia.

- Along the first axis (F_1), in the (F_1, F_2) diagram, it can be seen on the West side, that Light Rare Earth Element (LREE) are associated to R1, R2 and P2 (Liétard, 1977; Cases *et al*., 1982) order indexes

Table 7: Iron amount before and after DCB process

	Before DCB		After DCB
Samples	Fe_2O_3 (%)		Fe EPR (ppm)
G1	3.18	1.99	3561.5
G2	1.97	1.52	2522.3
G3	1.61	1.36	2465.4
G4	1.43	1.24	2107.2
G5	3.44	1.96	3026.1
G6	6.52	1.86	2784.1
G7	3.93	1.65	2614.5
G8	2.29	1.48	2726.7
G9	1.67	1.43	1737.9
G10	3.00	1.83	2211.3
G11	2.13	1.54	2772.8
G12	1.76	1.42	2481.9
G13	18.27	1.87	2713.1
G14	3.30	1.45	2099.3

Table 8: Numerical results of quantitative mineralogy

										Residues (%)			
	Kaolinite	Quartz	Anatase	Mica	Smectite	Goethite	Gibbsite	PF	Total				
Samples	(%)									Fe_2O_3	MgO	K_2O	H_2O
G1	53.19	12.58	2.76	5.71	11.6	2.90	9.59	2.45905	100.78905	0.00142	0.058	0.00027	1.09
G2	68.38	4.91	2.69	4.92	8.4	1.60	7.83	2.99385	101.72385	0.00434	0.042	4.0E-05	0.61
G3	79.87	1.43	2.65	3.65	4.8	1.29	5.21	3.3639	102.2639	0.00024	0.024	5.0E-05	0.45
G4	81.81	1.10	2.88	2.70	4.4	1.13	4.85	3.4218	102.2918	-0.00413	0.022	-1.0E-04	0.50
G5	51.74	12.46	2.78	6.03	11.2	3.19	10.73	2.4188	100.5488	0.00285	0.056	0.00011	1.05
G6	61.58	5.48	2.51	4.76	8.8	6.68	8.26	2.7561	100.8261	-0.0003	0.044	0.00012	1.04
G7	70.58	2.70	2.61	4.44	7.6	3.81	6.64	3.06225	101.44225	-0.00038	0.038	0.00028	0.88
G8	75.20	1.69	2.61	4.13	6.8	2.00	6.22	3.2206	101.8706	0.00037	0.034	-0.00019	0.62
G9	79.50	0.63	2.18	3.81	6.0	1.32	5.39	3.36555	102.19555	0.00539	0.030	-3.0E-05	0.43
G10	48.19	14.77	2.67	5.40	13.2	2.69	11.21	2.2952	100.4252	0.00303	0.066	-0.00020	1.08
G11	58.51	9.57	2.89	5.87	11.2	1.72	8.64	2.6493	101.0493	0.0005	0.056	0.00019	0.93
G12	68.32	4.67	2.83	5.24	8.8	1.35	7.22	2.98825	101.41825	0.0016	0.044	-0.00012	0.92
G13	51.04	0.00	2.27	4.38	11.69	19.69	9.96	2.45015	101.48015	0.0263	-0.0838	-0.11594	0.64
G14	75.86	0.02	2.36	3.33	7.2	3.14	6.77	3.25695	101.93695	-0.00081	0.036	0.00021	0.48

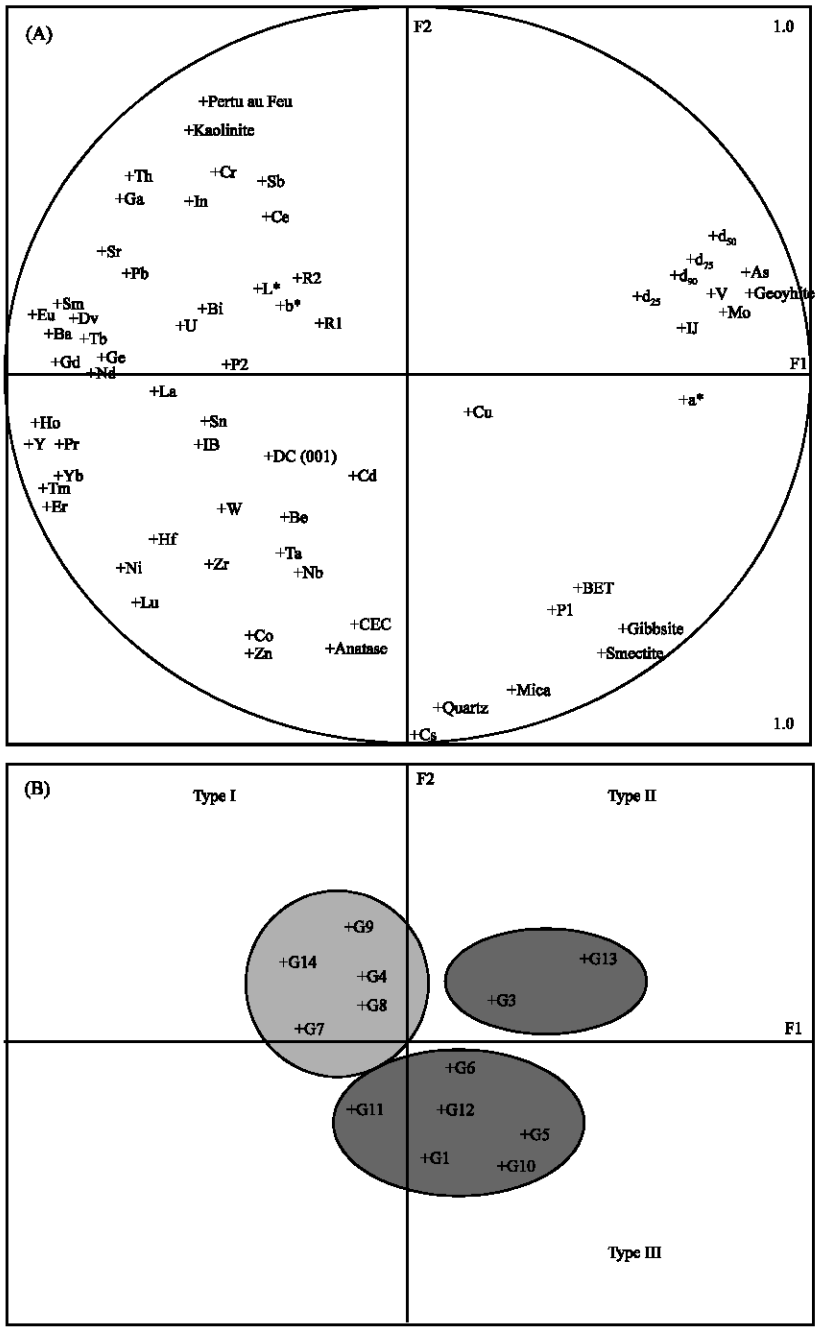

Fig. 4: Principal component analysis realised with physico-chemistry parameters on the 14 samples of Gounioubé. (A) projection of variables in the (F_1, F_2) plane and (B) projection of samples in the (F_1, F_2) plane

Toward the North West side of the diagram, the kaolinite amount is in normal dependence according to Loss On Ignition, the variation of which is correlated to chromium amount. This relation derives from a double effect: in this mineralogical association, kaolinite is a major mineral containing the highest equivalent of structure water and in addition, chromium traces are statistically correlated to structure disorders (Cases *et al*., 1982) that increase the fineness (Cases *et al*., 1986) and then the adsorbed water. Brightness and whiteness are also associated to this pole.

- On the Eastern side, the particle size characteristics (D_{25}, D_{50}, D_{75}, D_{90}), the gœthite amount and the yellow

index normally vary together. The correlation between the goethite amount and the yellow index results from the presence of gœthite in the coarser fractions which bring them a yellow coloration. The variations of molybdenium, vanadium and arsenic are, in part, correlated to those of gœthite

- On the southern side, the variations of mica are associated to the variations of quartz. This point is usual in secondary kaolins since during the transportation and the sedimentation process, both quartz and micas are mechanically sorted in the coarser fractions and then sediment in beds or levels where kaolinite, usually finer, is less abundant

To the South-West side, the smectite amount is correlated to the amount in gibbsite and the BET specific surface. This relation probably results from the fact that the external surface of smectites as described by nitrogen adsorption (Cases *et al*., 1992) is usually greater than the total specific surface of kaolinite (Cases *et al*., 1982). However the relation between gibbsite and smectites would be a little unusual considering a standard *in situ* lateritic alteration profile that concentrate gibbsite in the surface horizons and smectites in the deeper (Nguetnkam *et al*., 2008). Then this point may be the trace of a paleo-alteration before sedimentation, without posterior alteration.

On the Southern pole, The illite amount is associated with, rubidium and caesium What shows that both the elements are mainly associated to the mica-like fraction (the feldspar amount is very low) of the materials as suggested by the high statistical correlations between potassium on one hand and rubidium (Fig. 5) and caesium (Fig. 6) on the other hand. It must be also noticed that these statistical relations show a low dispersion and pass close to zero, what means that mica-like phase is the only significant vector of rubidium and strontium with constant Rb/K and Cs/K ratio.

It must be also noticed that the character to be rich in kaolinite is opposed to the BET surface.

At last, the usual relation between niobium and tantalum is observed (Fig. 7). The low dispersion of the distribution and the unique ratio Nb/Ta ≈ 12 reveal that the sediments derive from the same parent rocks or from rocks with the same niobiotantalites.

Typology: The projection of samples in the (F_1F_2) plane, (Fig. 4B) leads to a typology of Gounioubé samples. Then, it will be considered that the Gounioubé clays are out of three main types.

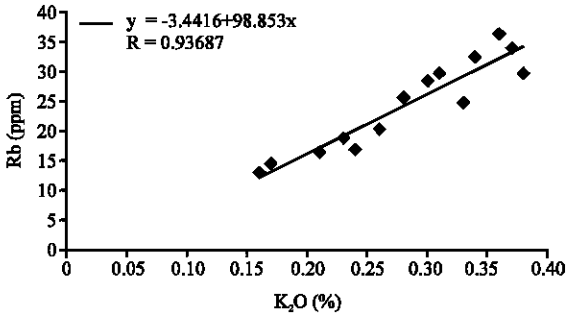

Fig. 5: Correlation between rubidium and potassium

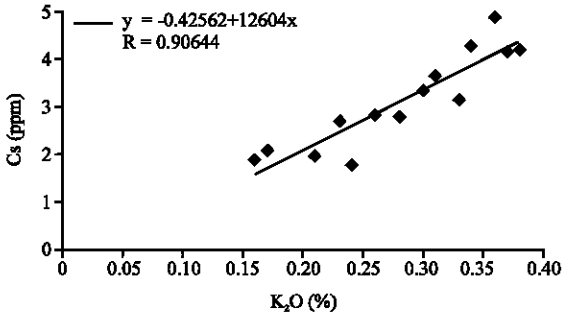

Fig. 6: Correlation between Caesium and potassium

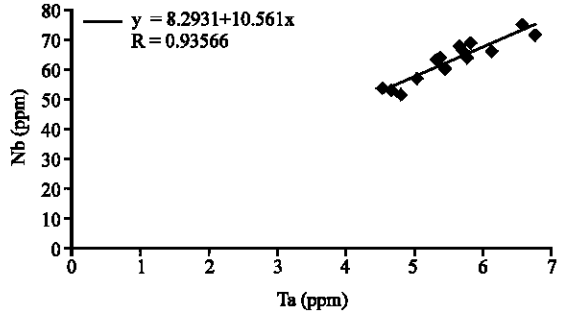

Fig. 7: Correlation between niobium and tantalum

- Type I is represented by samples G2, G4, G7, G8, G9 and G14 the main characteristic of which is the richness in kaolinite; G9 and G14 are the richest. They are white, very disordered, with specific surfaces lower than those of the others
- Samples G3 and G13 define the type II. They are coarse and their yellow colour results from the presence of iron under the form of gœthite
- The type III is represented by samples: G1, G5, G6, G10, G11 and G12. They are characterised by the presence of smectites and 10 Å d-spacing sheet-silicates, with the highest specific surfaces, compared to other samples

CONCLUSION

This typology reveals that the clays from Gounioubé deposit cannot be used as coating pigments for paper industry, due to their low cristallinity, the presence of smectites and their colour (type II) (Delon *et al*., 1982). To the contrary, types I an II, could be used in semi-reinforced rubber in applications where the colour is not a concern (Yvon *et al*., 1991, 2002). Great volume applications are certainly possible in cast or pressed ceramics for types I and III. The type II could be specifically dedicated to applications in terra cotta products (floor tiles, roof tiles, bricks, pottery) (Balavoine, 2002; Balavoine *et al*., 2003).

ACKNOWLEDGMENTS

This study was done in the Laboratoire Environnement and Mineralurgie (LEM) of Nancy. We are grateful to all of the members of the LEM for their contribution of this work. We also take this opportunity to thank the french government for financial support.

REFERENCES

Andji, Y.Y.J., 1998. Contribution to the mineralogical and physicochemical characterization of clays from Gounioubé. Ph.D. Thesis, Université de Cocody Abidjan (Côte d'Ivoire), pp: 154 (In French).

Andji, Y.Y.J., J. Sei, A. Abba Toure, G. Kra, D. Njopwouo, 2001. Mineralogical and physicochemical characterization of some clay samples of the site of Gounioube (Côte d'Ivoire). J. Soc. Ouest-Afr. Chim., 11: 143-166.

Balavoine, L., 2002. Typological analysis of raw materials of roofing tiles, prevision of the properties. Ph.D. Thesis, Institut National Polytechnique de Lorraine, Nancy, France, pp: 279 (In French).

Balavoine, L., J. Yvon and R. Cristancho, 2003. Typological analysis of raw materials for roofing tiles. Adv. Sci. Technol. Sci. New Technol. Silicate Ceramics, 34: 135-142.

Brunauer, S., P.H. Emmett and E. Teller, 1938. Adsorption of gases in multimolecular layers. J. Am. Chem. Soc., 60: 309-309.

Carignan, J., P. Hild, G. Mevelle, J. Morel and D. Yeghicheyan, 2001. Routine analyses of trace elements in geological samples using flow injection and low pressure on-line liquid chromatography coupled to ICP-MS: A study of geochemical reference materials BR, DR-N, UB-N, AN-G and GH. Geost. Newslett., 25: 187-198.

Cases, J.M., O. Liétard, J. Yvon and J.F. Delon, 1982. Crystallochemical, morphological and interfacial properties of disordered kaolinites. Bull. Min., 105: 439-457.

Cases, J.M., P. Cunin, Y. Grillet, C. Poinsignon and J. Yvon, 1986. Methods of analysing morphology of kaolinite: Relations between crystallographic and morphological properties. Clay Min., 21: 55-68.

Cases, J.M., I. Berend, G. Besson, M. François, J.P. Uriot, F. Thomas and J.E. Poirier, 1992. Mechanisms of adsorption and desorption of water vapour by homoionic montmorillonite: I the sodium exchange form. Langmuir, 8: 2730-2739.

Delineau, T., 1994. Clays of the Charentes basin (France): Typological and crystallochemical analysis, speciation of iron and applications. Ph.D. Thesis, Institut National Polytechnique de Lorraine, Nancy, France, pp: 627 (In French).

Delineau, T., T. Allard, J.P. Muller, O. Barrès, J. Yvon, J.M. Cases, 1994. FTIR reflectance vs. EPR studies of structural iron in kaolinites. Clays and Clay Min., 42: 308-320.

Delon, J.F., O. Liétard, J.M. Cases, M. Richard, G. Sauret and J.P. Maume, 1982. On the possibilities of coating paper and cardboard with kaolinic clays from Charentes. Bull. Min., 105: 571-581.

Dorthe, J.P., 1964. Study of the clay deposit in Gounioubé region. Company of Mining Development (SODEMI)-Côte d'Ivoire, Report No. 84, pp: 70 (In French).

Farmer, V.C., 1964. Infrared absorption of OH groups in kaolinite. Science, 145: 1189-1190.

Hogg, C., P. Malden and R. Meads, 1975. Identification of iron containing impurities in natural kaolinite using Mössbauer effect. Mineral. Mag., 40: 89-96.

Lebart, L., A. Morineau and J.P. Fénelon, 1979. Processing of statistical data. Methods and Programs. Dunod, (Ed.) Paris.

Liétard, O., 1977. Contribution to the study of the physico-chemical, cristallographic and morphological properties of kaolins. Ph.D. Thesis, Institut National Polytechnique de Lorraine, Nancy, France, pp: 345 (In French).

Mantin, I. and R. Glaeser, 1960. Fixation of the cobaltihexamine ions by the acid montmorillonites. Bull. Gr. Fr. Argiles, 12: 83-88.

Nguetnkam, J.P., R. Kamga, F. Villiéras, G.E. Ekodeck, A. Razafitianamaharavo and J. Yvon, 2005. Assessment of the surface areas of silica and clay in acid leached clay materials using concepts of adsorption on heterogeneous surfaces. J. Colloid Interface Sci., 289: 104-115.

Nguetnkam, J.P., R. Kamga, F. Villiéras, G.E. Ekodeck and J. Yvon, 2008. Pedogenic formation of smectite in a vertisol developed from granitic parent material in Kaélé (Cameroon, Central Africa). Clay Min., 42: 487-501.

Rémy, J.C. and L. Orsini, 1976. Use of the chloride of cobaltihexamine for the simultaneous determination of the capacity of exchange and the exchangeable bases of grounds. Sci. Soil., 4: 269-275.

Scherrer, P., 1918. Bestimmung der gröbe und der inneren struktur von kolloidteilchen mittels Röntgenstrahlen. Nachr. Ges. Wiss. Göttingen., 2: 96-100.

USGS. (United State Geological Survey), 2008. Mineral resources program. Commodity Statistics and Information.

Yvon, J., J. Baudracco, J.M. Cases and J. Weiss, 1990a. Elements of Quantitative Mineralogy in Microanalysis of Clays. In: Lay Materials, Structure, Properties and Applications, Decarreau, A. (Ed.). SFMC., Paris, ISBN: 2-903589-06-02, pp: 475-489 (In French).

Yvon, J., L. Michot, J.M. Cases and J.E. Poirier, 1990b. Industrial Applications of Clays: A Daily Pragmatism for the Cutting Edge Technologies. In: Clay Materials, Structure, Properties and Applications. Decarreau, A. (Ed.). SFMC., Paris, ISBN: 2-903589-06-02, pp: 495-509 (In French).

Yvon, J., Ph. Marion, L. Michot, F. Villieras, F.E. Wagner and J. Friedl, 1991. Development of mineralogy applications in mineral processing. Eur. J. Min., 3: 667-676.

Yvon, J., J.M. Cases, F. Villiéras, L. Michot and F. Thomas, 2002. Natural technical minerals: Knowledge, typology and properties of custom. C.R. Géosci., 334: 717-730.